# Supporting Information

## Flexible Conductive MXene/Cellulose Nanocrystal Coated Nonwoven Fabrics for Tunable Wearable Strain/Pressure Sensors

Qianming Li,[1#] Rui Yin,[1,2#] Dianbo Zhang,[1] Hu Liu,[1*] Xiaoyu Chen,[1] Yanjun Zheng,[1] Zhanhu Guo,[3] Chuntai Liu,[1*] and Changyu Shen[1]

[1]Key Laboratory of Materials Processing and Mold (Zhengzhou University), Ministry of Education; National Engineering Research Center for Advanced Polymer Processing Technology, Zhengzhou University, Zhengzhou, Henan 450002, China

[2]China Astronaut Research and Training Center, Beijing 100094, China

[3]Integrated Composites Laboratory (ICL), Department of Chemical & Biomolecular Engineering, University of Tennessee, Knoxville, Tennessee 37996, United States

*: *Correspondence authors*

E-mail address: liuhu@zzu.edu.cn (H. L.); ctliu@zzu.edu.cn (C. L.);

#: These authors contributed equally to this work.

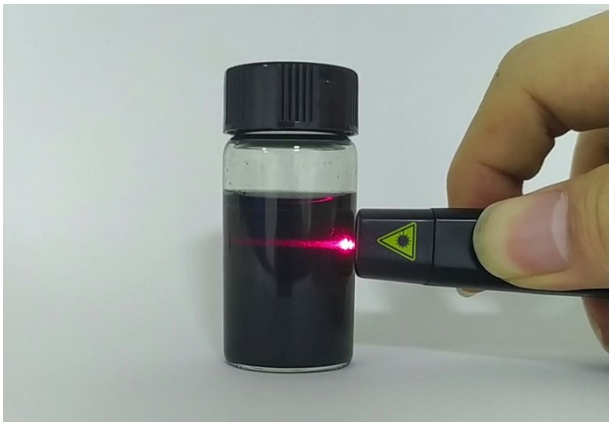

**Fig. S1** Tyndall effect of MC aqueous dispersion

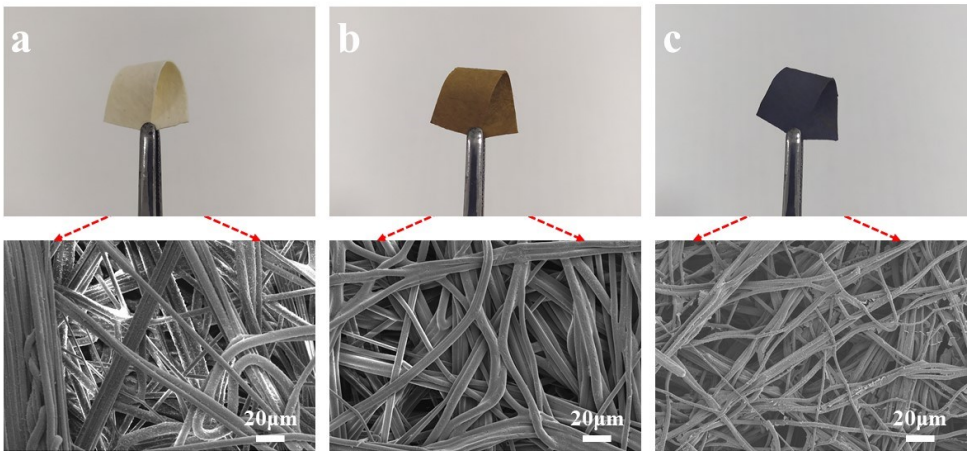


**Fig. S2** Photographs and SEM images of (a) original NWF, (b) *p*-NWF and (c) MC@*p*-NWF.

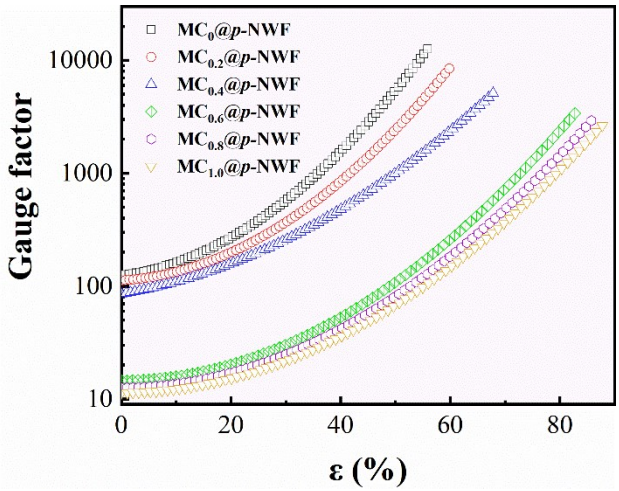


**Fig. S3** GF as a function of strain for different MC@*p*-NWF.

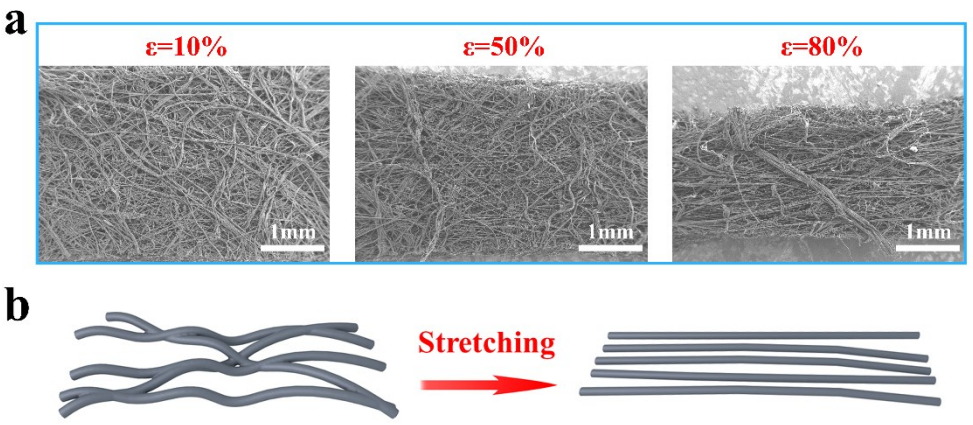


**Fig. S4** Schematic illustration (a) and in-situ SEM images (b) for the microstructural change of the strain sensor in the initial tension process.

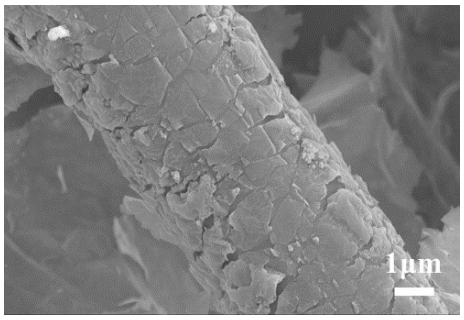


**Fig. S5** Surface SEM images of $MC_0$@*p*-NWF and its crack density is calculated to be about 0.8 $\mu m^{-2}$. (The crack density is defined as the number of discontinuous cracks per unit area in this study)


**Fig. S6** Strain sensing mechanism illustration for the sensor with different CNC loading during the tension process.

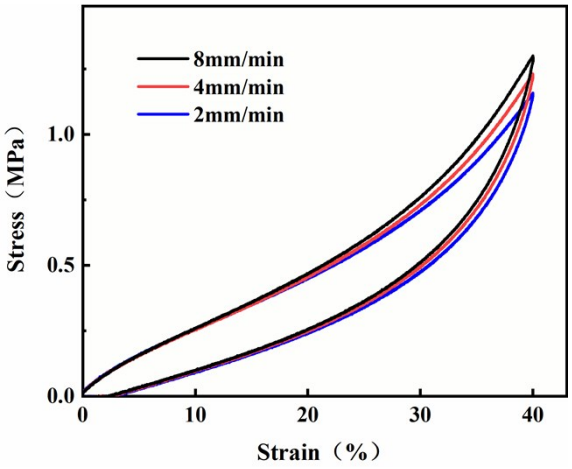


**Fig. S7** Stress-strain curves in the tensile tests.

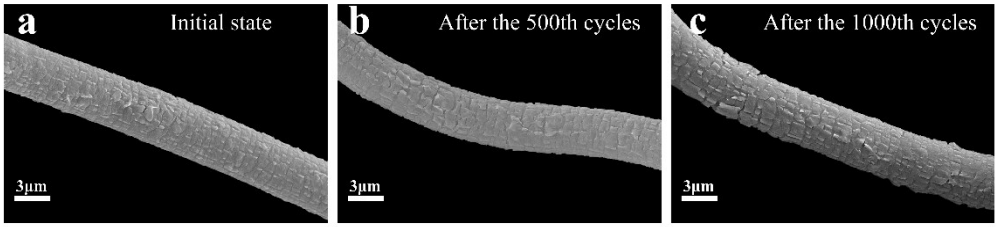


**Fig. S8** Surface SEM images of the sensor (a) at the initial state, (b) after the 500th and (c) after the1000th strain cycles.

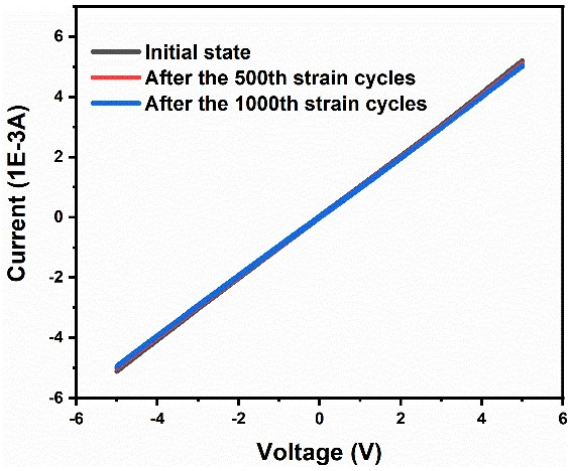


**Fig. S9** I -V curves of the sensor at the initial state and after the 500th/1000th strain cycles.

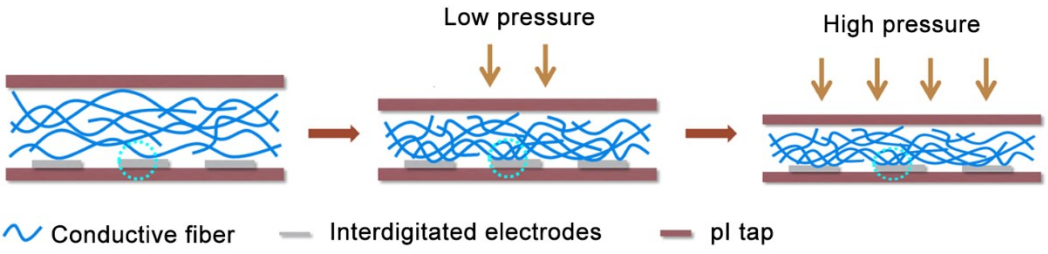


**Fig. S10** Schematic illustration for the microstructural change of the pressure sensor under low and high pressures.

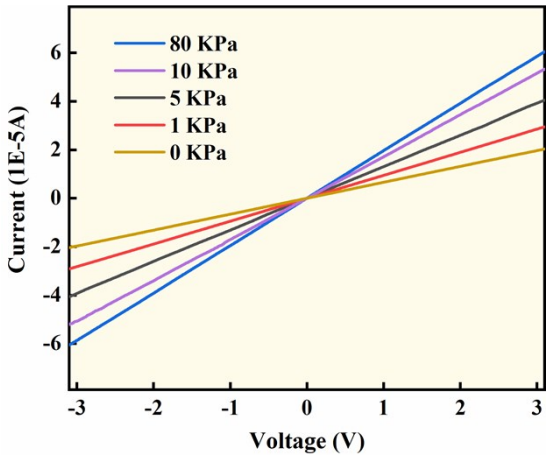


**Fig. S11** I-V curves of the pressure sensor at different external pressures.

**Tab. S1** The atomic ratio (C/O) of different materials

| Material | C atomic % | O atomic % | C/O atomic ratio |
|---|---|---|---|
| NWF | 82.67 | 15.83 | 5.22 |
| *p*-NWF | 72.72 | 23.20 | 3.13 |
| MC@*p*-NWF | 70.79 | 7.06 | 10.03 |